

E07-11-1120 Kaplan

Supplementary Figure 1 (S1). *unc-108(nu415)* mutant animals are hypersensitive (hic) to the cholinesterase inhibitor aldicarb. Aldicarb-induced paralysis for wild type, *unc-108(nu415)*, and *tomo-1(nu468)* animals was measured on NGM plates containing 1mM aldicarb (Sigma). *tomo-1(nu468)* mutant animals were used as a hic control strain. Data points show the mean of four trials (n=20 of each genotype/trial). Error bars represent SEM.

Supplementary Figure 2 (S2). Expression of FLAG-tagged UNC-108. (A) Western blot analysis, using an anti-FLAG antibody (Sigma), on lysed *unc-108(nu415)* worms expressing the *Pglr-1::UNC-108::FLAG* construct. (B) Stage four larval (L4) and young adult worms expressing the *Pglr-1::UNC-108::FLAG* construct were immunostained using an anti-FLAG antibody (Sigma), and imaged. (C) Individual red and green channel and overlay confocal images of double immunostained neuronal cell bodies of worms expressing *Pglr-1::UNC-108::FLAG* together with *Pglr-1::RFP::BET-1*. Scale bars are 10 μ m (ventral nerve cord) and 2 μ m (cell bodies)

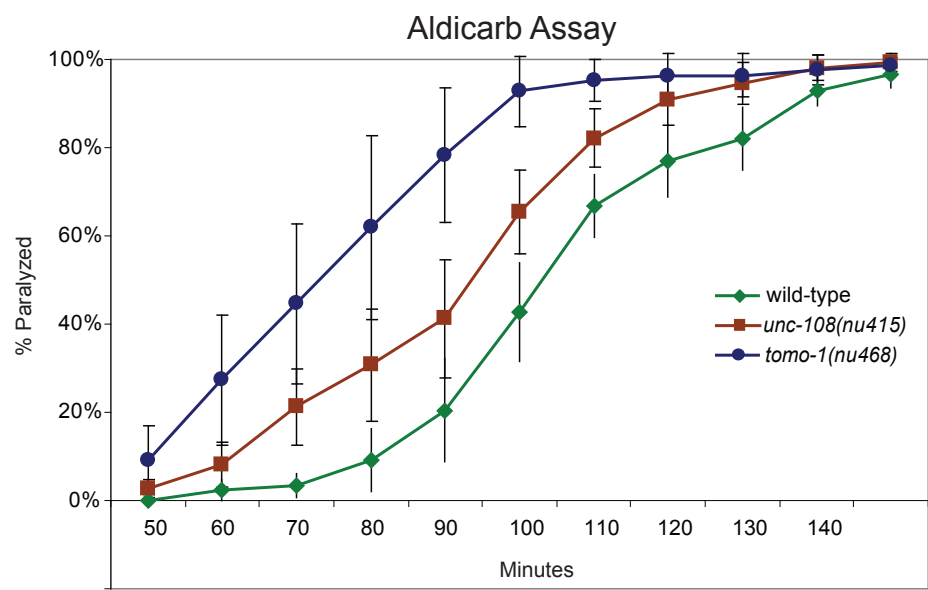
Supplementary Figure 3 (S3). GLR-1:GFP co-localization with intracellular compartment markers in *unc-108(nu415)* mutant neuronal cell bodies. Confocal images of PVC interneuron cell bodies are shown in *unc-108(nu415)* mutants. A single plane is shown for each cell. Individual red and green channel and overlay images are shown for GLR-1::GFP co-localization with the following RFP-tagged markers in *unc-108(nu415)* mutant animals: RFP::Rab5 (A), RFP::Rab14 (B), RFP::Rab11 (C), RFP::Rab10 (D), RFP::GOS-28 (E), and RFP::Syntaxin-16 (F). Scale bar is 2 μ m.

Supplementary Figure 4 (S4). Rationale and methodology for quantification of GLR-1::GFP co-localization with intracellular compartment markers. (A-B) Representative original and thresholded GLR-1::GFP images of wild type and *unc-108(nu415)* neuronal cell bodies are shown. (C-D) Graphs plotting pixel count against intensity (binned in 400 pixel increments) from the original images of wild type (C) and *unc-108(nu415)* neuronal cell bodies are shown with the same threshold (black dotted line) in both. The threshold was based on the region of interest (outlined in white in B) drawn around a GLR-1::GFP tubulovesicular structure in the *unc-108(nu415)* cell body. The pixel count plotted against pixel intensity for that region of interest is shown in light gray in (D) with the right y-axis corresponding to this data. The

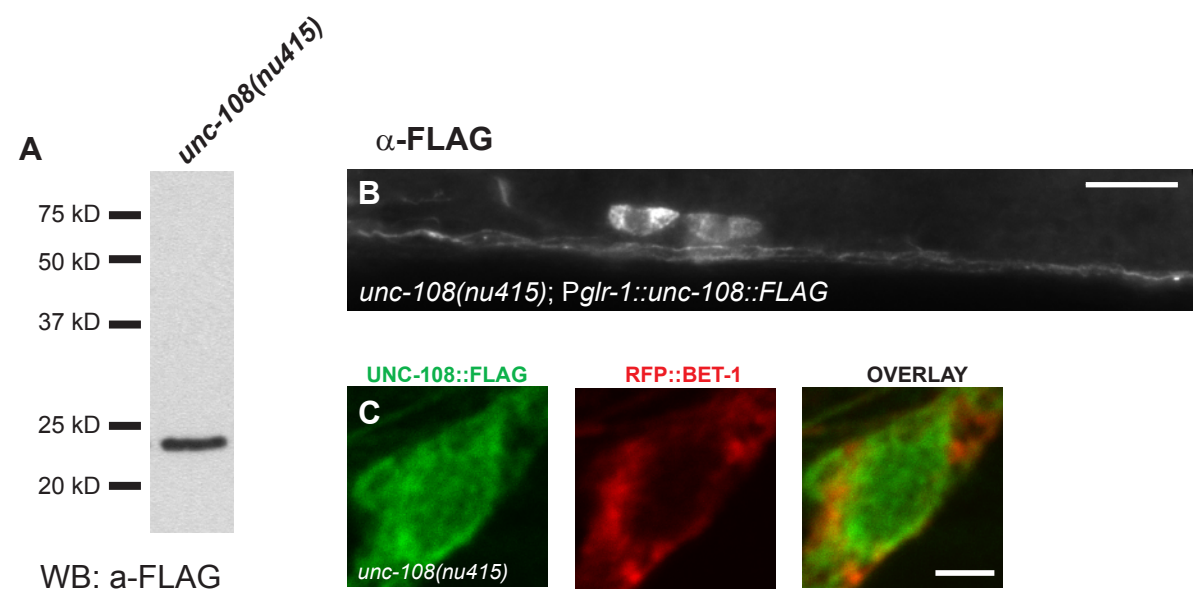
threshold (black dotted line) was calculated as one standard deviation below the average pixel intensity in this region of interest (light gray dotted line) (D). (E) The cumulative percent total pixel count for the original GLR-1::GFP wild type (gray line) and *unc-108(nu415)* (black line) cell body images was plotted against pixel intensity. Approximately 5% of the GLR-1::GFP pixels in the *unc-108(nu415)* cell body image were above the threshold set, whereas approximately 1% of the GLR-1::GFP pixels in the wild type cell body image using the same threshold. This indicates that the GLR-1::GFP tubulovesicular structures make up a large portion of the brightest 5% of pixels in *unc-108(nu415)* cell body images and that we can exclude background GLR-1::GFP fluorescence and include mainly the tubulovesicular structures by employing this method of thresholding. Scale bar is 2 μ m.

Supplementary Figure 5 (S5). Quantification of GLR-1::GFP co-localization with RFP::Syntaxin-13, RFP::Rab8, and ssTomato::KDEL in wild type versus *unc-108(nu415)* neuronal cell bodies. (A-B) Representative original and thresholded GLR-1::GFP, as well as RFP::Syntaxin-13, images of wild type and *unc-108(nu415)* neuronal cell bodies are shown. (C) Quantitative co-localization between thresholded GLR-1::GFP and RFP::Syntaxin-13 was significantly greater in *unc-108(nu415)* mutant neuron cell bodies (n=5) as compared to wild type (n=5) ($p = 0.00120$) . (C-D) Representative original and thresholded GLR-1::GFP, as well as RFP::Rab8, images of wild type and *unc-108(nu415)* neuronal cell bodies are shown. (F) Quantitative co-localization between thresholded GLR-1::GFP and RFP::Rab8 was significantly greater in *unc-108(nu415)* mutant neuron cell bodies (n=5) as compared to wild type (n=5) ($p = 7.07 \times 10^{-4}$) . (G-H) Representative confocal images of individual red and green channels and overlay of GLR-1::GFP and ssTomato::KDEL in wild type and *unc-108(nu415)* neuronal cell bodies. (I) There was no significant difference in co-localization between minimally thresholded GLR-1::GFP and ssTomato::KDEL *unc-108(nu415)* mutant neuron cell bodies (n=5) as compared to wild type (n=5) ($p = 0.349$) . The average percent co-localization of GLR-1::GFP with ssTomato::KDEL in wild type (66.9 +/- 3.09 %) and *unc-108(nu415)* mutant (65.5 +/- 1.59%) neuron cell bodies was consistent with both our and previously published results (Grunwald *et al.*, 2003) showing that ~65% of GLR-1::GFP is retained in the ER based on Endo H-sensitivity assays. Scale bar is 2 μ m, error bars represent SEM, and values that differ significantly from wild type (by Student's t-test) are indicated as follows: p<0.01 (*) or p<0.001 (**).

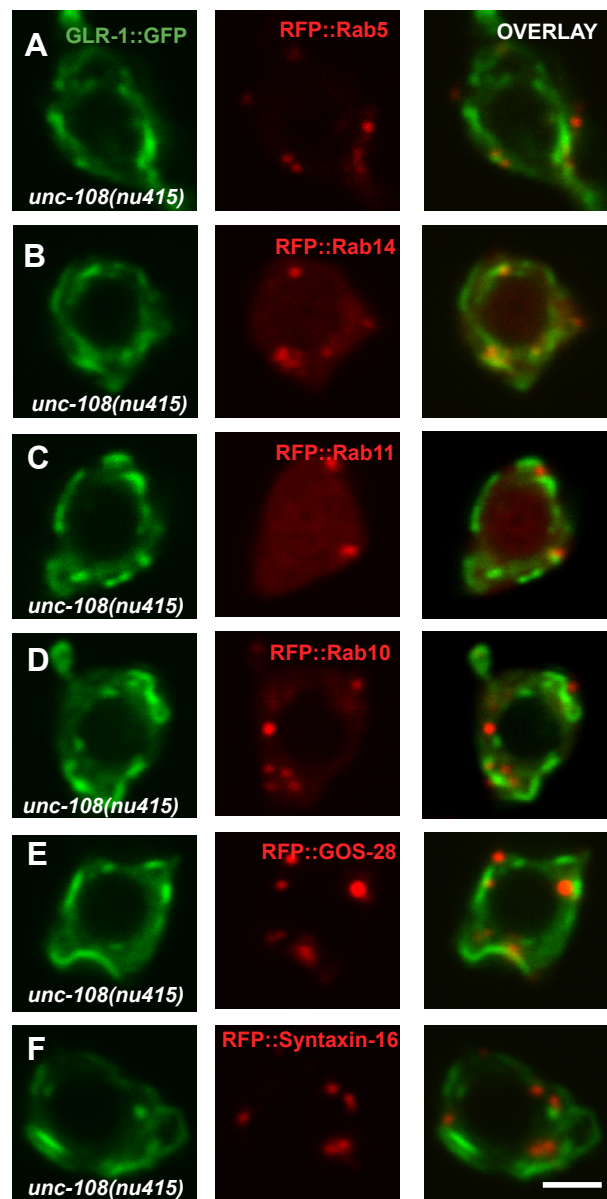
Supplementary Figure 1 (S1)



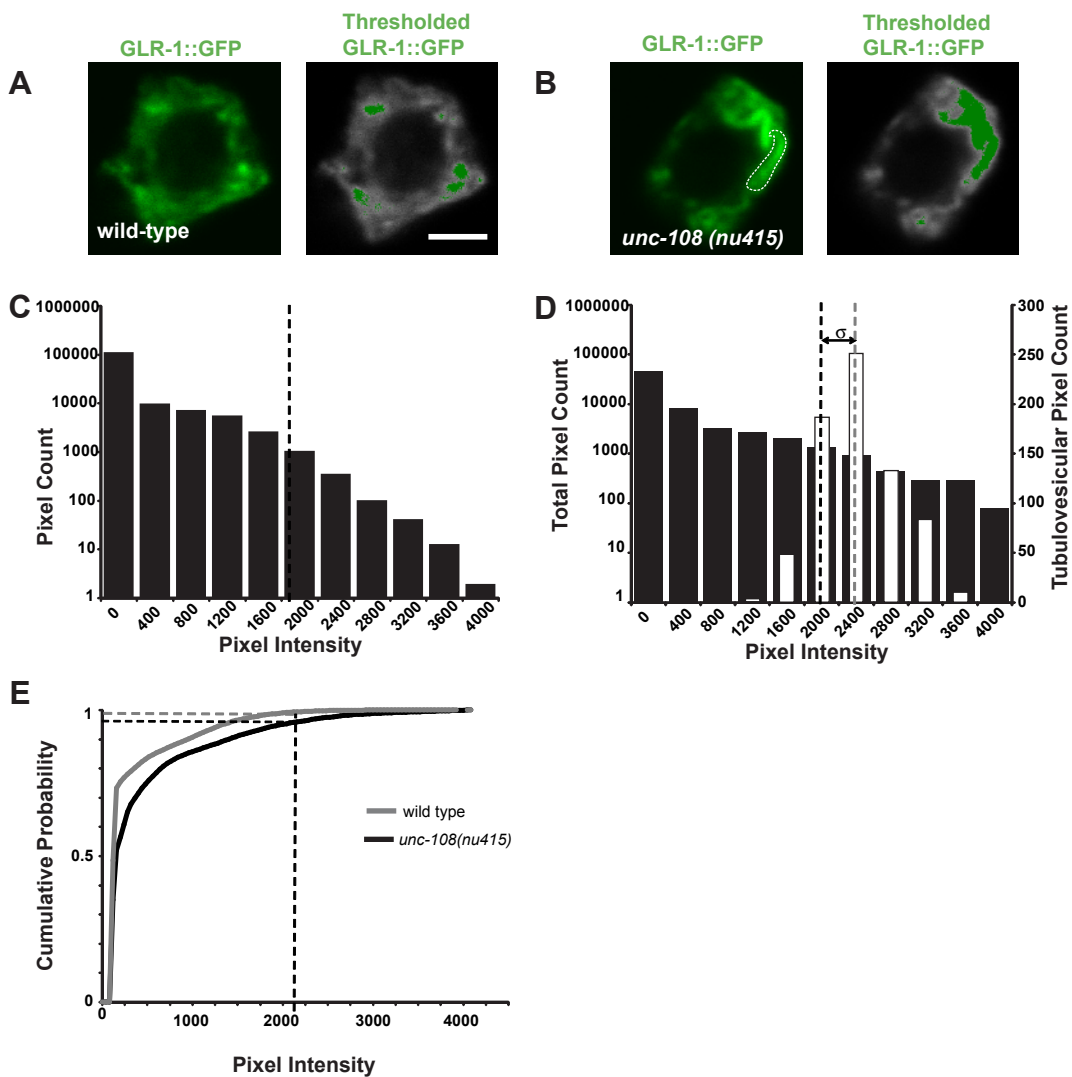
Supplementary Figure 2 (S2)



Supplementary Figure 3 (S3)



Supplementary Figure 4 (S4)



Supplementary Figure (S5)

